Optics Communications 399 (2017) 87–97

Contents lists available at ScienceDirect

Optics Communications

journal homepage: www.elsevier.com/locate/optcom

Imaging quality evaluation method of pixel coupled electro-optical imaging system

Xu He[a,*], Li Yuan[a,b], Chunqi Jin[a,b], Xiaohui Zhang[a]

[a] Changchun Institute of Optics, Fine Mechanics and Physics, Chinese Academy of Sciences, Changchun 130031, China
[b] Graduate University of Chinese Academy of Sciences, Beijing 100039, China

ARTICLE INFO

OCIS codes:
060.2350
060.2270
110.4850
120.4800

Keywords:
Fiber-optic image bundles
Evaluation of imaging quality
Modulation transfer function
Pixel coupling error
Oscillation convergence

ABSTRACT

With advancements in high-resolution imaging optical fiber bundle fabrication technology, traditional photoelectric imaging system have become "flexible" with greatly reduced volume and weight. However, traditional image quality evaluation models are limited by the coupling discrete sampling effect of fiber-optic image bundles and charge-coupled device (CCD) pixels. This limitation substantially complicates the design, optimization, assembly, and evaluation image quality of the coupled discrete sampling imaging system. Based on the transfer process of grayscale cosine distribution optical signal in the fiber-optic image bundle and CCD, a mathematical model of coupled modulation transfer function (coupled-MTF) is established. This model can be used as a basis for following studies on the convergence and periodically oscillating characteristics of the function. We also propose the concept of the average coupled-MTF, which is consistent with the definition of traditional MTF. Based on this concept, the relationships among core distance, core layer radius, and average coupled-MTF are investigated.

Results show that the coupled-MTF oscillation converges to a fixed value when the deviation between a spatial frequency of input signal and Nyquist frequency is 1% and when the total number of pixels in the coupled system is more than 1000. The minimal frequency deviation corresponds to the slow velocity of the oscillational convergent. The oscillation amplitude of coupled-MTF differs in tangential and sagittal directions in a manner related to the corresponding pixel coupling error. The coupled-MTF periodically oscillates with the alignment error between the coupled pixel. One cycle is equivalent to the diameter of fiber cladding. The observation from the simulations further reveal that the distance between adjacent fiber cores and the dimension of core layer are directly related to the system imaging quality and the signal-to-noise ratio. Moreover, the average coupled-MTF can be used to quantitatively describe the function of related parameters and the imaging quality of the system.

1. Introduction

Numerous single fibers can be arranged in accordance with a certain rule and form a fiber-optic image bundle to transmit image information, such as fiber-optic image bundles that have good arrangement quality, 1024×768 resolution, Φ 6 μm cladding diameter, and visible to near-infrared spectral range [1]. Comprehensive performance can be improved by adding fiber-optic image bundles to a traditional imaging system. For example, adding fiber-optic image bundles to a Raman imaging system can improve signal-to-noise ratio (SNR) [2]. The scale of an optical system can be greatly reduced by using fiber-optic image bundles coupled with array detector in a high-performance ultra-wide-angled lens [3]. Combining fiber-optic image bundles in a hyperspectral imager can also considerably enhance the side width of slices [4].

However, a two-level coupled discrete sampling system becomes involved when fiber-optic image bundles are added to an optical imaging system with an array CCD. This limits the application of the traditional mathematical methods for MTF. First, the coupling error of the pixels leads to the difficulty of mathematic derivation based on Fourier transform. Second, for multistage discrete sampling systems, the transmittance of intensity at different coordinates of the array is different because of the coupling error of the pixels. Therefore, the applicability of the MTF cascade multiplication and spatial invariant assumption is no longer valid. These theoretical difficulties of traditional imaging quality evaluation models entail substantial research work. For instance, Donald et al. [5] experimentally investigated the influence of fiber-optic image bundles on the imaging quality of optoelectronic circuits. Seki et al. [6] reported the relationship of single fiber radius in the bundles with the imaging quality of a photoacoustic

* Corresponding author.
E-mail address: hexu_ciomp@sina.com (X. He).

http://dx.doi.org/10.1016/j.optcom.2017.04.029
Received 10 November 2016; Received in revised form 10 April 2017; Accepted 11 April 2017
Available online 02 May 2017

imager. Ford et al. [7] discussed the issue of system imaging quality evaluation after fiber-optic image bundles are added to the swept-source optical coherence tomography (OCT) from the angle of the SNR and resolution. MTF can indicate the characteristics of imaging system responses to different spatial frequency domains. For example, oblique-edge scanning method is used to evaluate the coupled sampling system with fiber-optic image bundles and CCD [8], or a cascade multiplication method is still applied to calculate the MTF of a two-stage coupled discrete sampling system [9]. Other studies have been based on the output light intensity distribution of grayscale cosine distribution signal from the coupled discrete sampling systems and have discussed the model of MTF according to its definitions [10–13]. This concept aims to prevent discrete coupling characteristics from interfering with transfer function calculation. The coupling contrast transfer function (CTF) between line-array fiber-optic image bundles and linear CCD is derived on the basis of the definition of CTF [14]. Related experiments have also revealed new features different from traditional CTF. To extend its application in hyperspectral remote sensing fields, we extensively investigated the coupled-MTF of pixels between an array of fiber-optic image bundles and CCD. A mathematical model of the coupled-MTF of a two-stage discrete sampling system and an initial-position average coupled-MTF was established. Some new characteristics of the function were also analyzed. Our study provided a theoretical basis for the optical design of fiber-optic imaging system and subsequent experimental verification.

2. Model and calculation

The main model of photoelectric imaging system using an array fiber-optical image bundle is shown in Fig. 1. This model includes an optical telescope, array fiber-optical image bundles, a coupling objective lens, and CCD array.

The principle sketch involves the front-telescope system, which obtains the object image (λ1–λ2) to the focal plane at a certain magnification. Fiber-optic image bundles do not change their numerical aperture (N.A.), and the optical fiber core diameter is considerably greater than the radius of an Airy-disk radius of a telescope system. The coupling lens is used to couple with an optical fiber beam output image to CCD. The input window of the fiber-optic image bundle is arranged on the focal plane of the telescope lens. Moreover, the output window of the bundle is positioned on the object surface of the coupling objective lens. The CCD-sensitive surface is located on the imagine focal plane of the coupling objective lens.

The ideal situation is shown in Fig. 2(a). The diameter of a single fiber of a bundle is the same as the pixel size of CCD, hence allowing for one-to-one coupling. The imaging quality of the whole imaging system

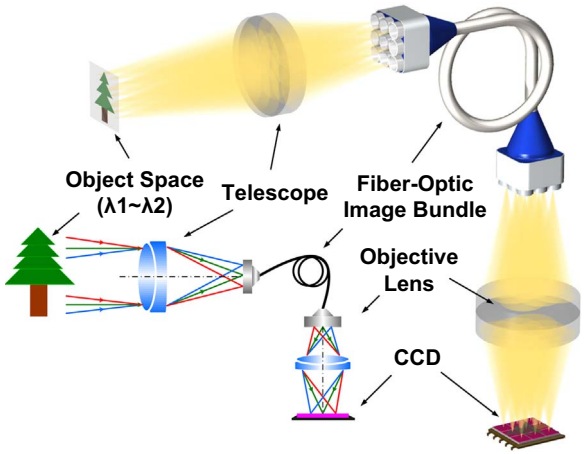

Fig. 1. Principle of the array fiber-optic image bundles.

agrees with the theoretical design. However, the actual alignment of the imaging system introduces pixel alignment error. A coupling error exists between the pixels of the fiber bundle and the CCD (Fig. 2(b)). Consequently, the imaging quality of the system changes compared with the theoretical situation.

The R in Fig. 2 represents the radius of the fiber cladding, whereas r represents the radius of the fiber core. Δi and Δj represent the pixel coupling deviations in the tangential and sagittal directions, respectively, δ denotes the initial positional deviation between the grayscale cosine distribution target and the pixel coupling array. We define the "coupled modulation transfer function" (coupled-MTF) of the system according to the output response of the system to the input signal of the grayscale cosine distribution to avoid the limitation of the spatial invariant assumption. The physical model is shown in Fig. 3.

The optical target of the grayscale cosine distribution enters the telescope imaging system after a two-time discrete sampling of the fiber-optic image bundle and the CCD. Finally, the target image is obtained in accordance with the grayscale level and its distribution of each pixel. The modulation depth of the output image can be calculated by using the concept of statistical averages. Then, we develop the coupled-MTF mathematical model of the coupled discrete sampling system through the intensity modulation definition. In addition, the cosine signal is oriented in two directions orthogonal to each other in the coupled-MTF model system. As such, the MTF model of the coupled discrete sampling system in the tangential and sagittal directions is established.

We should explain the simplified section before the detailed derivation of the coupled-MTF expression. (1) The actual coupling deviation exists in three-dimensional space. The coupling error with six free dimensions between the coupled systems is existent. However, the defocusing errors and tilt errors in three-dimension can be controlled to sub-micron and sub-second order by the traditional method. The accuracy of this magnitude can be ignored for the output image quality for 1000×1000 coupled pixels. (2) The telescope and coupling objectives are traditional optical system. Hence, the MTF (f) in each field of view is the fixed value. (3) The long-distance transmission of the laser through the fiber introduces strong Gaussian characteristics of output signal. However, the fiber-optic image bundles mentioned in the paper is only used for the image transmission of wide spectral (350–750 nm). Moreover, the input beam itself does not have Gaussian characteristics. Therefore, the Gaussian characteristics of the output beam caused by the optical fiber transmission can be neglected [15]. Therefore we assume that each individual fiber in the bundles only integrally transmits the intensity distribution of the input beam rather than changing it within a single fiber. (4) The reference indicates that a large crosstalk in the fiber bundle is present when used to transmit laser beam. The crosstalk rate is generally −60 dB to −10 dB when the fiber bundle length is 100 m or more, whereas the fiber-optic image bundles mentioned in the paper are only used for wide spectral image transmission within a very short distance. In this case, the decrease of modulation caused by crosstalk is less than 1% [16,17], and the crosstalk rate is close to the fixed value. Therefore, in the following mathematical derivation, C is defined as the degree of modulation decrease caused by the average crosstalk rate in the fiber bundle.

First, the intensity cosine distribution target is used for the input signal. In this case, the signal distribution in the input window of the optical fiber is

$$I(x) = 1 + C_0(f)\cos(2\pi f(x + \delta)) \tag{1}$$

where, f, $C_0(f)$, and δ are the spatial frequency, modulation, and initial positional deviation of the input signal, respectively. With the Nyquist frequency $f_N = 1/(4R)$, the intensity of the output signal of any row i and column j pixel in the fiber array is given by

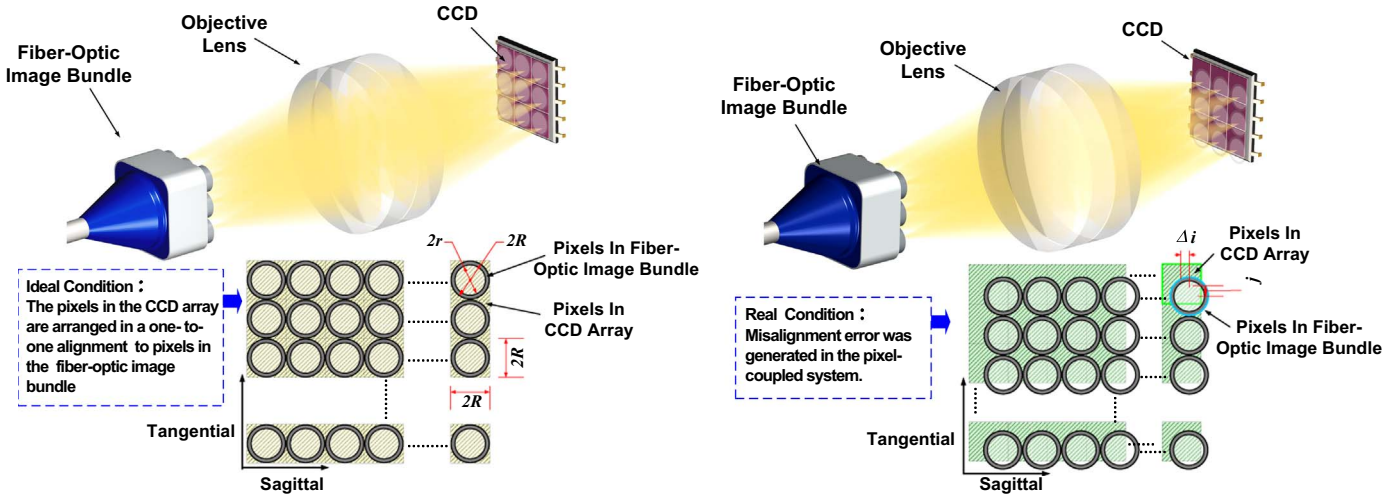

Fig. 2. Schematic diagram of the coupling principle of array fiber-optic image bundles and array CCD detector. (a) Theory of the one-to-one coupled state of the pixels (b) Pixel-coupling state with alignment errors.

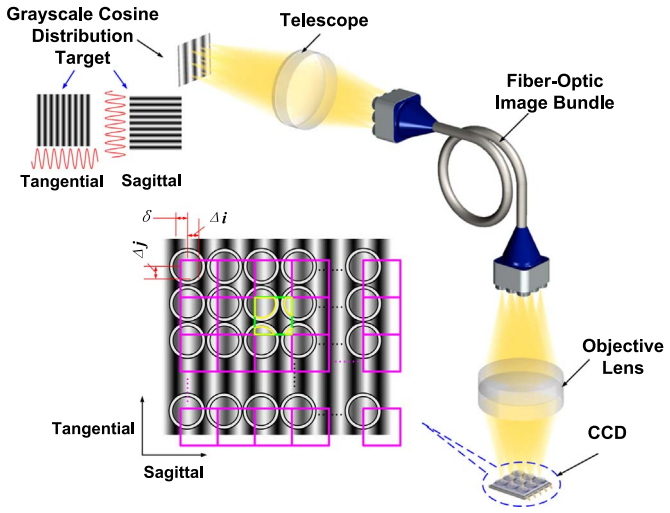

Fig. 3. Method of the MTF evaluation model of the coupled discrete sampling system.

$$\begin{aligned} I'_{i,j}(x) &= 2\int_{x_j-r}^{x_j+r}(1+C_0(f,\delta)\cos(2\pi f\,(x+\delta)))(r^2-(x-x_j)^2)^{1/2}dx \\ &= 2\int_{2jR-r}^{2jR+r}(1+C_0(f,\delta)\cos(2\pi f\,(x+\delta)))(r^2-(x-2jR)^2)^{1/2}dx \end{aligned} \tag{2}$$

A sketch of the coupling situation between the pixel of the fiber bundles and CCD is shown in Figs. 4 and 5. The mathematical model is derived for these two kinds of situations according to the analysis of alignment error.

In the first case, the coupling error between the pixel of CCD and fiber-optic image bundle array only allows a single CCD pixel to receive

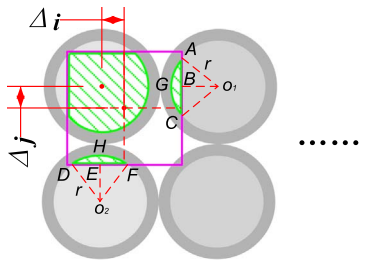

Fig. 4. Diagram of the first kind of pixel coupling error.

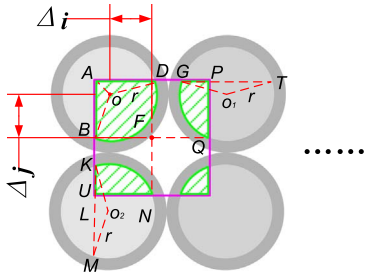

Fig. 5. Diagram of the second kind of pixel coupling error.

the optical signal from three adjacent optical fiber pixels (Fig. 4). Considering the radius difference between the fiber core and the cladding, we can obtain the following relationship,

$$\sqrt{(R-\Delta i)^2+(R-\Delta j)^2} \geq r. \tag{3}$$

Then, a bow of light intensity receive area “AGCB” is obtained as follows:

$$S_{AGCB} = r^2\arccos\frac{R-\Delta_i}{r} - (R-\Delta_i)\times\sqrt{r^2-(R-\Delta_i)^2}. \tag{4}$$

A bow “DHEF” is shown below.

$$S_{DHFE} = r^2\arccos\frac{R-\Delta_j}{r} - (R-\Delta_j)\times\sqrt{r^2-(R-\Delta_j)^2} \tag{5}$$

The effective area of the output light intensity of the adjacent pixels is expressed as

$$\begin{aligned} S_{i,j} &= \pi r^2 - S_{i+1,j} - S_{i,j+1}, \\ S_{i,j+1} &= r^2\arccos\frac{R-\Delta_i}{r} - (R-\Delta_i)\times\sqrt{r^2-(R-\Delta_i)^2}, \\ S_{i+1,j} &= r^2\arccos\frac{R-\Delta_j}{r} - (R-\Delta_j)\times\sqrt{r^2-(R-\Delta_j)^2}. \end{aligned} \tag{6}$$

In the presence of the first kind of coupling deviation, the expression of the intensity of the output signal of the random i and j pixels in the CCD array is

$$I''_{i,j} = \frac{S_{i,j}}{\pi r^2}I'_{i,j} + \frac{S_{i+1,j}}{\pi r^2}I'_{i+1,j} + \frac{S_{i,j+1}}{\pi r^2}I'_{i,j+1}. \tag{7}$$

The $I'_{i,j}$ in Eq. (7) represents the output light intensity of the No. i and j fibers, and $I''_{i,j}$ is the expression of the output light intensity of the No. i and j CCD pixels in the detector.

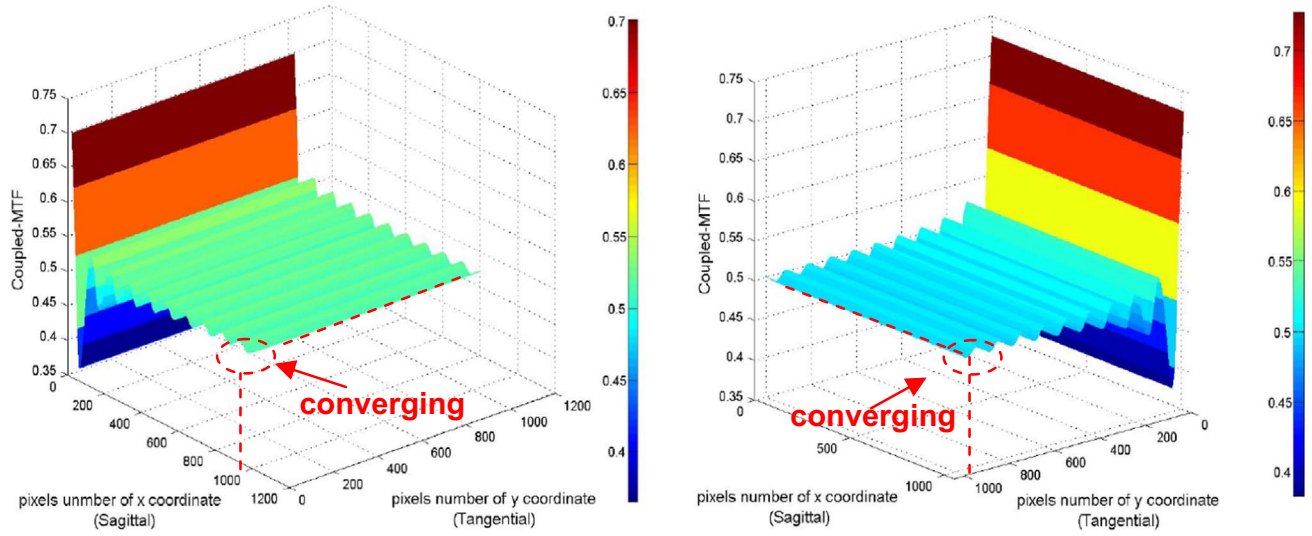

(a) Simulation of the oscillation convergence of the coupled-MTF in the sagittal direction

(b) Simulation of the oscillation convergence of the coupled-MTF in the tangential direction

Fig. 6. Simulations of the oscillation convergence of the coupled-MTF with the number of pixels in the array at a deviation of cosine target spatial frequency and Nyquist frequency of 1%. (a) Simulation of the oscillation convergence of the coupled-MTF in the sagittal direction. (b) Simulation of the oscillation convergence of the coupled-MTF in the tangential direction.

In the second case, the coupling error between the pixel of CCD and fiber bundles enables a single CCD pixel to receive an optical light intensity from four adjacent optical fiber pixels (Fig. 5). Similar to the calculation deduced above, the light transmission area of the four adjacent fibers in the bundle is deduced as the following geometric relations:

$$\begin{aligned} S_{i,j} &= S_{ABFD} = S_{\triangle OAB} + S_{\triangle OAD} + S_{OBFD} \\ &= \frac{(\sqrt{r^2-(R-\Delta i)^2}+R-\Delta j)\times(R-\Delta i)}{2} \\ &\quad + \frac{(\sqrt{r^2-(R-\Delta j)^2}+R-\Delta i)\times(R-\Delta j)}{2} \\ &\quad + \frac{r^2}{2}\left(\frac{3\pi}{2} - \arccos\frac{R-\Delta j}{r} - \arccos\frac{R-\Delta i}{r}\right) \end{aligned} \tag{8}$$

$$S_{i,j+1} = \sqrt{r^2-(R-\Delta j)^2}\times(R-\Delta j) + r^2\left(\pi - \arccos\frac{R-\Delta j}{r}\right) - S_{i,j} \tag{9}$$

$$S_{i+1,j} = \sqrt{r^2-(R-\Delta i)^2}\times(R-\Delta i) + r^2\left(\pi - \arccos\frac{R-\Delta i}{r}\right) - S_{i,j} \tag{10}$$

$$S_{i+1,j+1} = \pi r^2 - S_{i,j} - S_{i,j+1} - S_{i+1,j} \tag{11}$$

In the second kind of coupling deviation, the expression of the output signals from the random i and j pixels in the CCD is expressed by:

$$I''_{i,j} = \frac{S_{i,j}}{\pi r^2} I'_{i,j} + \frac{S_{i+1,j}}{\pi r^2} I'_{i+1,j} + \frac{S_{i,j+1}}{\pi r^2} I'_{i,j+1} + \frac{S_{i+1,j+1}}{\pi r^2} I'_{i+1,j+1}. \tag{12}$$

Based on Eqs. (1), (2), (7), and (12), and on the intensity modulation definition of the MTF, we can deduce the coupled-MTF of the system, as shown in Eq. (13):

$$coupled-MTF(f,\Delta i,\Delta j,\delta) = C\cdot\frac{\frac{1}{M}\sum_{i=1}^{M} I''_{\max i,j}(f,\Delta i,\Delta j,\delta) - \frac{1}{N}\sum_{i=1}^{N} I''_{\min i,j}(f,\Delta i,\Delta j,\delta)}{\frac{1}{M}\sum_{i=1}^{m} I''_{\max i,j}(f,\Delta i,\Delta j,\delta) + \frac{1}{N}\sum_{i=1}^{N} I''_{\min i,j}(f,\Delta i,\Delta j,\delta)}/C_0(f). \tag{13}$$

The Δi in Eq. (13) represents the pixel coupling error of the sagittal direction (Δi=R-OC), and Δj represents the pixel coupling error of the tangential direction (Δj=R−OE). M indicates the number of pixels in the CCD with an output signal larger than the value of adjacent pixels, and N indicates the number of pixels in the CCD with an output signal less than that of the adjacent pixels. For the coupled discrete sampling system, the coupled-MTF of the system is no longer a fixed value at a given spatial frequency but related to the coupling deviation along the two directions between the array fiber-optic image bundle and the CCD. Furthermore, MTF is also correlated to the total number of pixel in the array, as well as the initial position deviation between the cosine signal and fiber array. The law can be derived by mathematical simulation method.

3. Simulations and discussion

3.1. Convergence of the coupled-MTF

As mentioned above, when the grayscale cosine distribution optical object is used as input signal, the target generating precision is difficult to guarantee. Thus, we first study the convergence of the coupled-MTF nearby the Nyquist frequency domain.

(1) One of our simulation conditions: optical fiber cladding radius R of 3 μm, core layer radius r of 2.5 μm; the fiber-optic image bundles of 1024×1024; the initial position deviation of 15% R; the pixel coupling error along the x and y directions as 25% R and 55% R, respectively; and the spatial frequency of the input cosine target as 99% of the Nyquist frequency (f=0.99f_N). Given Eq. (13), the simulation results of the oscillation convergence of the coupled-MTF is obtained with the number increasing of pixels in the array

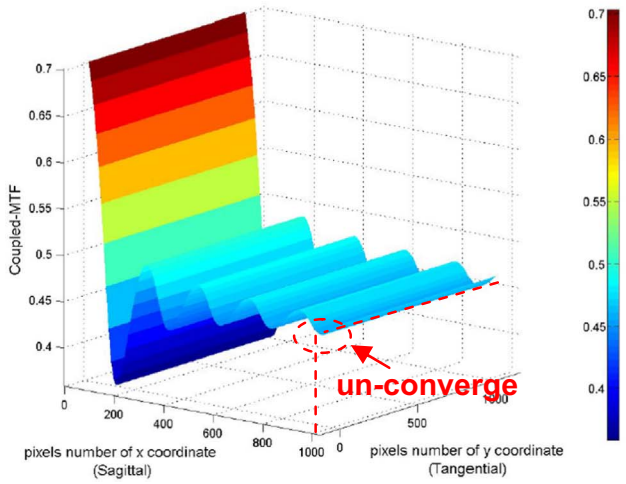

(a) Simulation of the oscillation convergence of the coupled-MTF in the sagittal direction

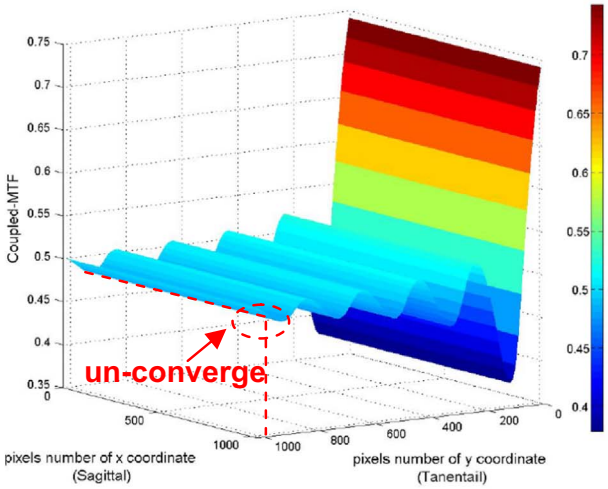

(b) Simulation of the oscillation convergence of the coupled-MTF in the tangential direction

Fig. 7. Simulations of the oscillation convergence of the coupled-MTF with the number of pixels in the array at a deviation of cosine target spatial frequency and Nyquist frequency of 0.5%. (a) Simulation of the oscillation convergence of the coupled-MTF in the sagittal direction. (b) Simulation of the oscillation convergence of the coupled-MTF in the tangential direction.

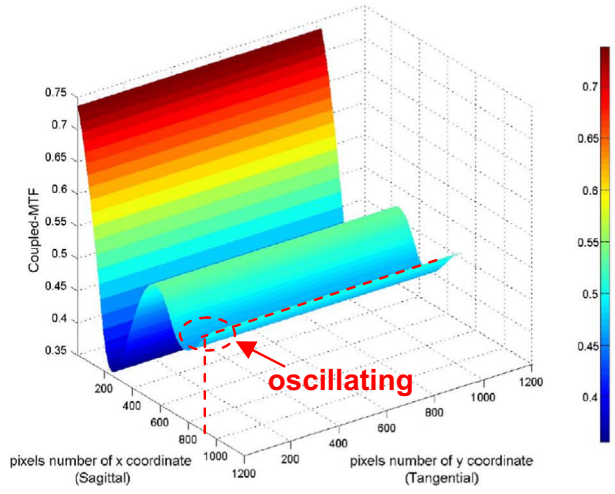

(a) Simulation of the oscillation convergence of the coupled-MTF in the sagittal direction

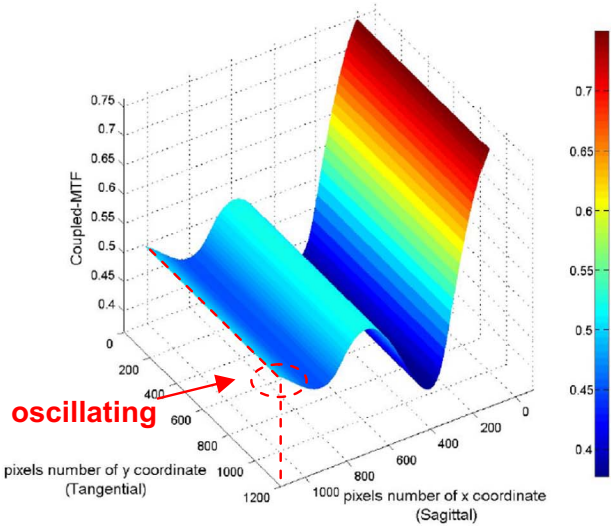

(b) Simulation of the oscillation convergence of the coupled-MTF in the tangential direction

Fig. 8. Simulations of the oscillation convergence of the coupled-MTF with the number of pixels in the array at a deviation of cosine target spatial frequency and the Nyquist frequency of 0.2%. (a) Simulation of the oscillation convergence of the coupled-MTF in the sagittal direction. (b) Simulation of the oscillation convergence of the coupled-MTF in the tangential direction.

(Fig. 6). The simulation of the oscillation convergence of the coupled-MTF in the sagittal direction is shown in Fig. 6(a), and the simulation in the tangential direction is shown in Fig. 6(b).

(2) When the fiber-optic image bundle, the CCD parameters, and coupling deviation are similar to those of the first case, and the deviation of the spatial frequency is 0.5%, we simulate the oscillation convergence of the coupled-MTF in the sagittal and tangential directions (Fig. 7(a) and (b)).

(3) When the fiber-optic image bundle, CCD parameters, and the coupling deviation are similar to those of the first case, and the deviation of the spatial frequency is 0.2%, the simulations of the oscillation convergence of the coupled-MTF are shown as follows (Fig. 8).

(4) When the fiber-optic image bundle, CCD parameters, and coupling deviation are similar to the first case, and the deviation of the cosine target spatial frequency and the Nyquist frequency is 0.1%, the simulation of the oscillation convergence of the coupled-MTF in the sagittal and tangential directions with the number increasing of pixels in the array is shown in Fig. 9(a) and (b).

As revealed by the simulation results for the coupled discrete sampling system, composing of array CCD and fiber-optic image bundles, the MTF differs in the sagittal and tangential directions with

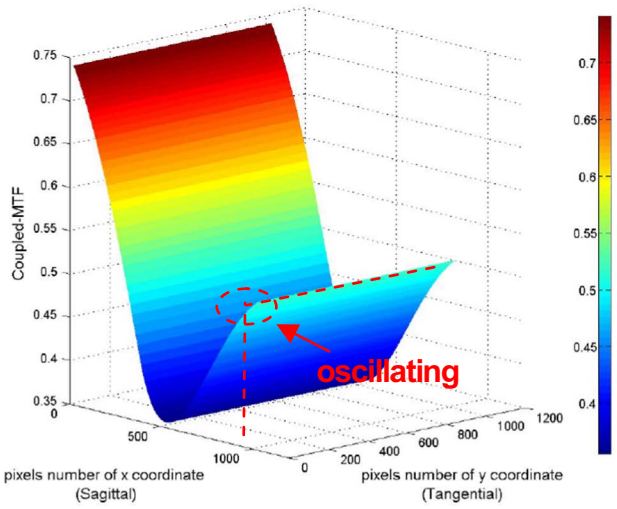

(a) Simulation of the oscillation convergence of the coupled-MTF in the sagittal direction

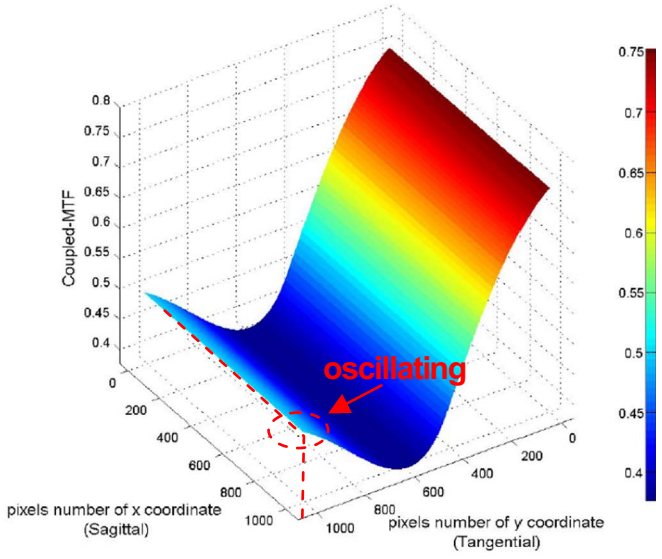

(b) Simulation of the oscillation convergence of the coupled-MTF in the tangential direction

Fig. 9. Simulations of the oscillation convergence of the coupled-MTF with the number of pixels in the array at a deviation of cosine target spatial frequency and the Nyquist frequency is 0.1%. (a) Simulation of the oscillation convergence of the coupled-MTF in the sagittal direction. (b) Simulation of the oscillation convergence of the coupled-MTF in the tangential direction.

the same spatial frequency. The value of the coupled-MTF is related to the pixel coupling error in the two directions.

Regardless of sagittal or tangential direction of the coupling discrete system, the value of coupled-MTF is not determined under the following conditions: the pixel coupling error and initial position deviation are present; the spatial frequency of input cosine signal and the Nyquist frequency involve a small error. The coupled-MTF value is related to the total number of pixels in the system. When the number of pixels in the system increase, the value of the coupled-MTF oscillational convergent is fixed. The oscillational convergence rate of the coupled-MTF is related to the deviation of the spatial frequency. Particularly, the smaller differences between the spatial frequency of input signal and Nyquist frequency result in slower oscillational convergence rates of the coupled-MTF.

The pixel coupling deviation differs in the sagittal and tangential directions. Hence, the final convergence value of the coupled-MTF in the sagittal or tangential directions is different, as well as the fixed value of the oscillation also differs. However, the oscillation convergence trend of the coupled-MTF in the sagittal and tangential directions remains constant with the increase in total pixel number in the array.

When the other parameters are determined, the oscillation convergence rate of the coupled-MTF in the tangential direction (or sagittal direction) of the coupled discrete system is related to the deviation of the spatial frequency (Fig. 10). For example, the spatial frequency deviation is 99%, and the total number of pixels exceeds 5000×5000 under the above simulation conditions, as shown in Fig. 10. The coupled-MTF oscillation amplitude is less than 0.001, approaching a stable fixed value. The coupled-MTF oscillation amplitude is approximately 0.01 when the spatial frequency deviation is 99.8%. Coupled-MTF oscillation converges to 0.003 only when the total number of pixels reaches 10,000×10,000. Whereas the coupled-MTF

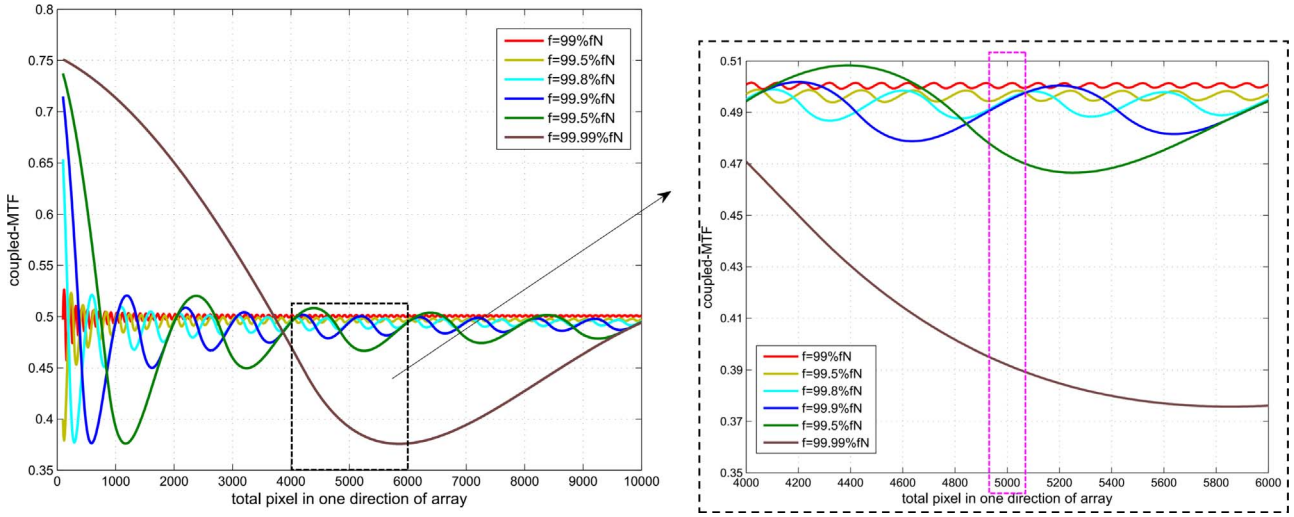

Fig. 10. Simulation of the deviation relation between the convergence rate of the coupled-MTF in the tangential direction and the input cosine signal spatial frequency.

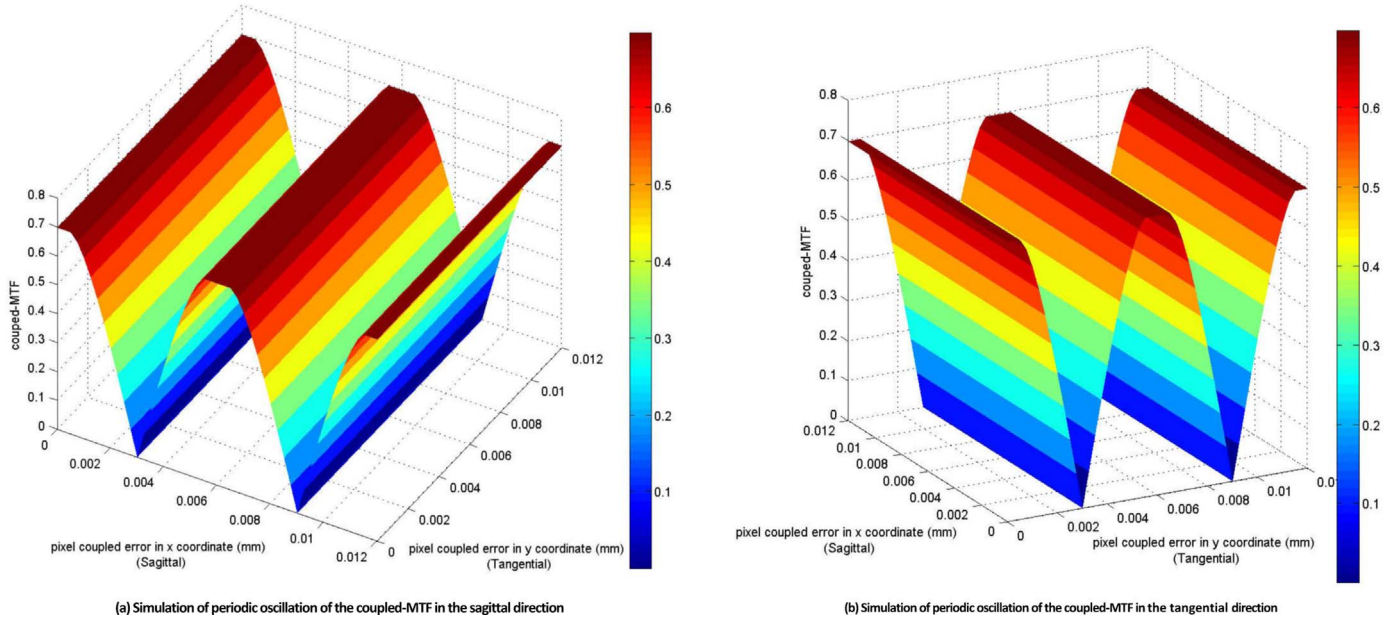

Fig. 11. Variation in the coupled-MTF with the pixel alignment error at a deviation of cosine target spatial frequency and Nyquist frequency of 0.25%. (a) Simulation of periodic oscillation of the coupled-MTF in the sagittal direction. (b) Simulation of periodic oscillation of the coupled-MTF in the tangential direction.

oscillation amplitude is close to 0.1 when the spatial frequency deviation is 99.99% and when the array contains 5000×5000 pixels. In addition, the coupled-MTF does not converge to a fixed value even if the total number of pixels reaches 10,000×10,000.

3.2. Pixel coupling deviation of the coupled-MTF

Limited by alignment accuracy, a pixel coupling error always exists between the fiber-optic image bundle and CCD. We then investigate the relation between the coupling-MTF and the alignment error between pixels based on Eq. (13).

(1) We assume a fiber cladding radius R of 3 μm, core layer radius r of 2.5 μm, optical fiber array of 1024×1024, initial positional deviation of 25% R, change in pixel coupling error along two directions from 0 R to 4 R, and spatial frequency of the input cosine target of 99.75% of the Nyquist frequency (f=0.9975f_N). The simulation results of the coupled-MTF with pixel coupling error in the sagittal and tangential directions can be obtained in accordance with Eq. (13) (Fig. 11).

(2) When the fiber-optic image bundle, CCD parameters, and the initial position deviation are similar to those of the first case, and the deviation of the spatial frequency of the input cosine target and the Nyquist frequency is 1%, the simulation results in the sagittal and tangential directions are those shown in Fig. 12.

(3) When the fiber-optic image bundle, CCD parameters, and initial position deviation are similar to the first conditions, and the deviation of the spatial frequency of the input cosine target and the Nyquist frequency is 2%, the simulation results are those shown in Fig. 13.

The simulation results show that when a small error exists between

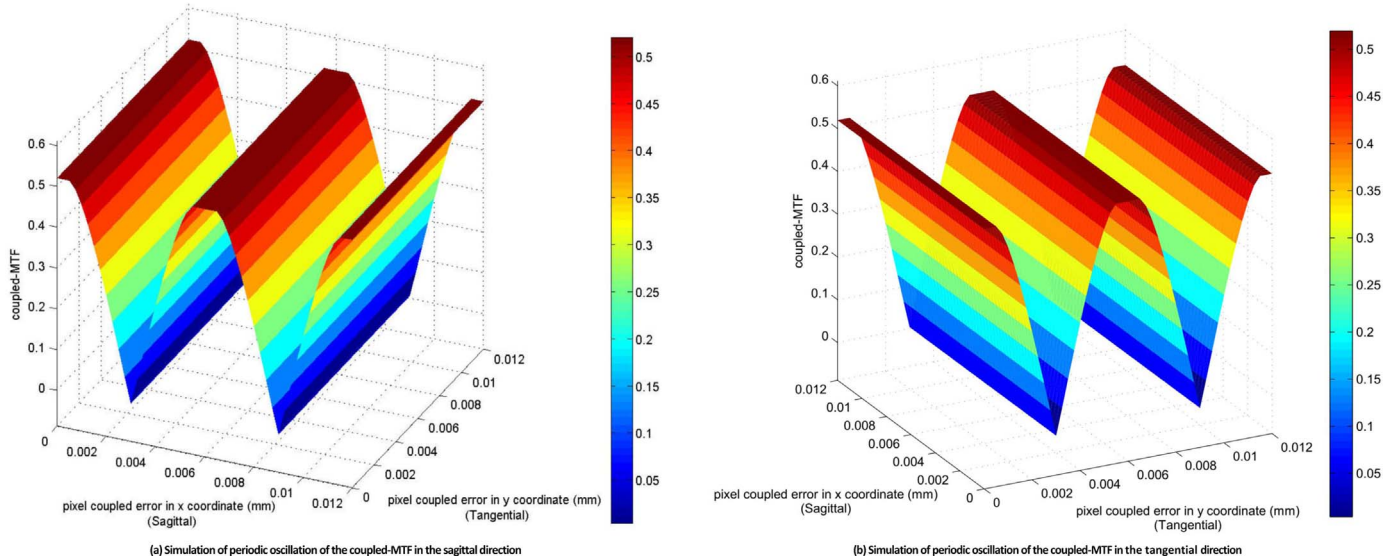

Fig. 12. Variation in the coupled-MTF with the pixel alignment error at a deviation of cosine target spatial frequency and Nyquist frequency of 1%. (a) Simulation of periodic oscillation of the coupled-MTF in the sagittal direction. (b) Simulation of periodic oscillation of the coupled-MTF in the tangential direction.

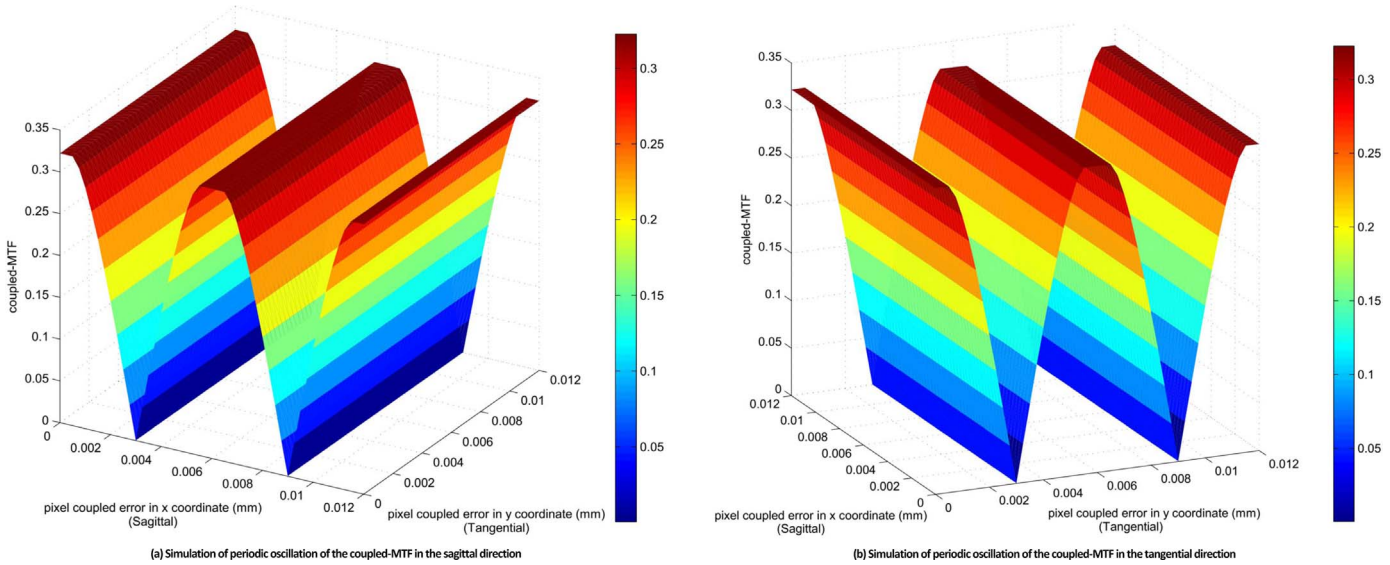

Fig. 13. Variation in the coupled-MTF with the pixel alignment error at a deviation of cosine target spatial frequency and Nyquist frequency of 2%. (a) Simulation of periodic oscillation of the coupled-MTF in the sagittal direction. (b) Simulation of periodic oscillation of the coupled-MTF in the tangential direction.

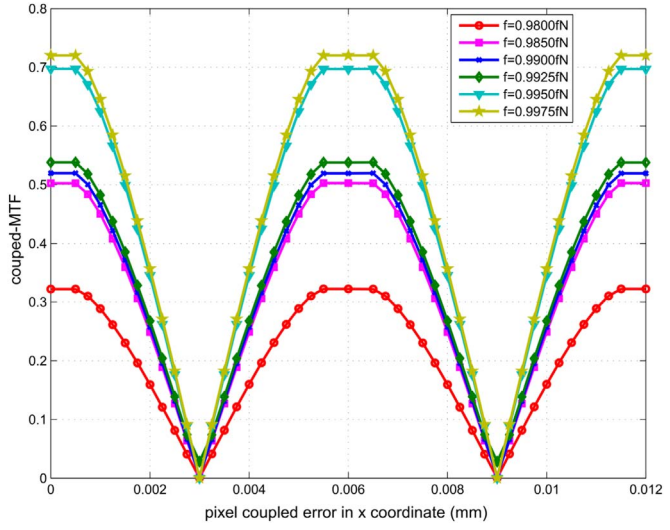

Fig. 14. Periodic oscillation simulation of the coupled-MTF value with pixel alignment error.

the spatial frequencies of the input cosine signal from the Nyquist frequency, the coupled-MTF in the sagittal and tangential directions periodically oscillates with the coupling error. The oscillation spatial period is the distance between two adjacent fibers, which is equal to twice the radius of the optical fiber cladding (2 R). Moreover, smaller deviations of the spatial frequencies generate larger oscillation amplitudes of the coupled-MTF with pixel coupling error. In addition, when the frequency deviation is determined, the minimum value of the coupled-MTF appears when the pixel coupling error is equal to the radius of the optical fiber cladding, and its value is close to zero when the effect introduced by crosstalk is ignored. The periodic oscillation characteristics of coupled discrete sampling system with pixel coupling error exist in the sagittal and tangential directions simultaneously.

The coupled-MTF oscillates with the pixel coupling error in the tangential (or sagittal) direction of the coupling system in accordance with the same period (Fig. 14). The amplitude of the oscillation is positively correlated to the deviation of the input cosine signal and the Nyquist frequency.

The above-mentioned simulation results indicate that the difference in pixel coupling error in the sagittal or tangential directions of the array led to the different transfer function values corresponding to the two directions. In the presence of a small deviation between the spatial frequency of the input grayscale cosine distribution signal and the Nyquist frequency, the MTF of the system oscillation converged with the increase in pixel number. Moreover, the oscillation is convergent and periodic with the pixel coupling error.

4. Calculation of the average coupled-MTF

For a coupled discrete imaging system composed of an array fiber-optic image bundle and an array CCD, the imaging quality of the system is determined by the pixel size of the CCD, the cladding radius of the optical fiber, and the diameter of the core layer. The dimension of pixel in array CCD and the distance between random adjacent fiber cores in the bundles are primary factors affecting the theoretical image quality of the system. We then analyze and discuss the influence of different parameters on the imaging quality of the coupled system to provide basis for the design and optimization of similar systems. However, simulation results based on Eq. (13) show that the initial positional deviation between the grayscale cosine distribution target and the coupled discrete system affects the convergence of the transfer function. Furthermore, Eq. (13) cannot completely evaluate the image quality of a coupled discrete sampled imaging system. For this reason, the model of average coupled-MTF is deduced for evaluating the image quality of the system, which is defined based on statistical average.

According to Eq. (13), K is the given initial positional deviations δ_k from the oscillation period 2 R of the coupled-MTF. In addition, the K functions of coupled-MTF(f, Δi, Δj, and δ_k) can be calculated for different initial positional deviations correspondingly. Similarly, the sagittal and tangential directions of pixel coupled error (Δi and Δj) are equal probability random errors. Hence, these directions can take H and T values in their oscillation period (2 R) and then statistical average. Subsequently, we defined the mean value of these functions as the expression of the average coupled-MTF as follows:

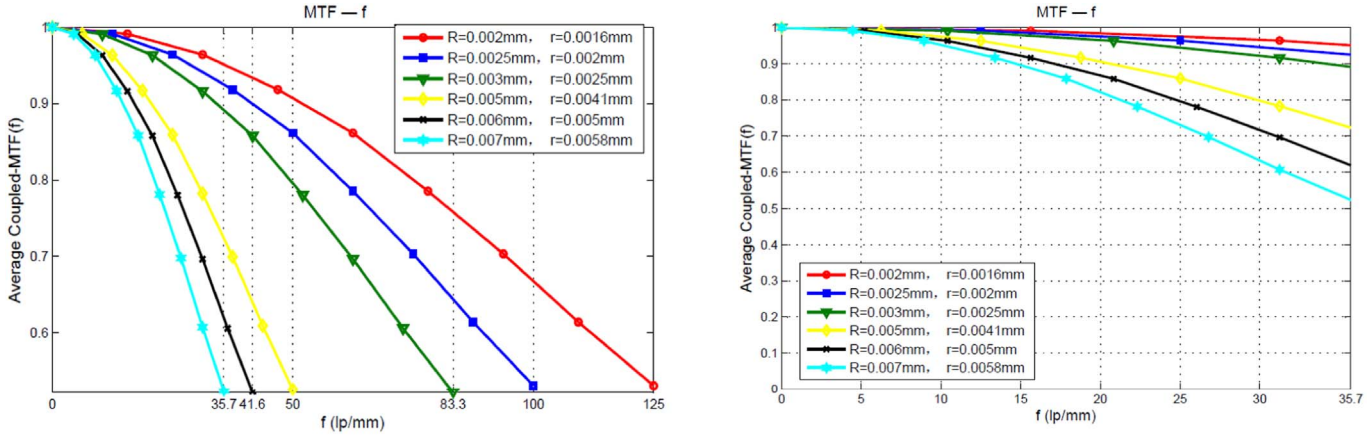

(a) Simulation curve of the average coupled-MTF in Nyquist frequency domain **(b) Simulation curve of the average coupled-MTF in the low frequency region**

Fig. 15. Simulation curve of the average coupled-MTF with different cladding radii in the Nyquist frequency domain. (a) Simulation curve of the average coupled-MTF in Nyquist frequency domain. (b) Simulation curve of the average coupled-MTF in the low frequency region.

Table 1
Effect of different cladding radii on the average coupled-MTF value.

R (mm)	Nyquist frequency	MTF (f), f=35.7 lp/mm
0.002	125(lp/mm)	0.956
0.0025	100(lp/mm)	0.922
0.003	83.3(lp/mm)	0.886
0.005	50(lp/mm)	0.723
0.006	41.6(lp/mm)	0.614
0.007	35.7(lp/mm)	0.522

$$coupled - MTF(f)_{average} = \frac{\left[\frac{1}{H\cdot K\cdot T}\cdot\sum_{h=0}^{H}\sum_{t=0}^{T}\sum_{k=0}^{K} C\cdot\frac{\frac{1}{M}\sum_{i=1}^{M} I''_{\max i,j}(f,\Delta ih,\Delta jk,\delta_k)-\frac{1}{N}\sum_{i=1}^{N} I''_{\min i,j}(f,\Delta ih,\Delta jk,\delta_k)}{\frac{1}{M}\sum_{i=1}^{m} I''_{\max i,j}(f,\Delta ih,\Delta jk,\delta_k)+\frac{1}{N}\sum_{i=1}^{N} I''_{\min i,j}(f,\Delta ih,\Delta jk,\delta_k)}\right]}{C_0(f)} \quad (14)$$

After the statistical average of the equal probability errors, the average coupled-MTF is independent of the initial position deviation and pixel coupled error between the fiber-optic image bundle and array CCD. Eq. (14) shows that the average coupled-MTF is only a function of the spatial frequency f, which is consistent with the definition of the MTF of the traditional space invariant system. The MTF(f) of the coupled discrete sampling system can be simulated by Eq. (14). R and r still represent the optical fiber cladding and core layer radius. The CCD pixel size is 2 R ×2 R, and the total number of pixels is 1024×1024.

The simulation results in Fig. 15 indicate that for a coupled discrete sampling image system consisting of a fiber-optic image bundle and a CCD, the average coupled-MTF can be used to characterize the imaging quality of the system. The cut-off frequency of the average coupled-MTF is determined by the dimension of optical fiber and the CCD pixel. When the distance of adjacent fiber cores, namely, the ratio of the radius of the optical fiber cladding to the core layer, reaches a certain value, a greater cladding radius would generate a lower cut-off frequency of the average coupled-MTF. In the middle- and low-frequency regions, the average coupled-MTF value is reduced. The selection of the cladding radius and the corresponding CCD pixel size considerably influence the ultimate resolution of the system and the overall imaging performance in the middle- and low-frequency regions (Table 1).

Therefore, investigating the effect of the ratio of the fiber cladding radius to the core layer radius on the average coupled-MTF is necessary. We assume that the optical fiber cladding radii are 0.003 and 0.006 mm, which suggest that the distance between adjacent fiber cores in the bundle is equal to these values. In some case, the fiber bundles are manufactured that the cladding is the material that holds the cores together. Hence, the definition of the distance between adjacent fiber cores is stricter. In addition, the differences between the cladding radii and core layer radii are 33%, 26%, 20%, 13%, and 6.7%. The simulation results are shown in Fig. 16(a) and (b).

The simulation results in Fig. 16 show that the distance of the adjacent fiber cores and its corresponding CCD pixel size are determined. Choosing different fiber core layer radii would not change the cut-off frequency of the coupled discrete sampling system but will affect the value of MTF at the cut-off frequency. Larger ratios between the deviation of the cladding and the core radii result in higher values of the average coupled-MTF at the cut-off frequency. However, the difference is not significant when the above ratios are 33% and 6.7%. The transfer function value at the Nyquist frequency and the difference between the values are shown in Table 2.

According to the comparison in Table 2, the deviation of the ratio of core distance and core radius has a lesser effect on the value of MTF of a coupled discrete imaging system. The effect on the limit resolution of the system is not significant. However, selecting a small core layer radius will greatly affect the transmission efficiency and SNR of the system.

5. Conclusion

An instrument can become “flexible” when fiber-optic image bundles are added to traditional optical imaging systems. Therefore, the flexibility and design redundancy of an optical path layout are improved. Moreover, the volume and weight of a photoelectric instrument are reduced, and the performance of the imaging systems is enhanced. With improvement in the manufacturing of fiber-optic image bundles, new optical imaging systems involving fiber-optic image bundles can be applied to various fields, including astronomy, military affairs, and microscopic imaging.

However, the MTF model based on Fourier transform and cascade multiplication theory shows some limitations affected by a two-stage discrete sampling effect and existence of pixel coupled error. This paper introduced a mathematical model of the coupled-MTF and the average coupled-MTF. Furthermore, the mathematical model is established by deriving the grayscale distribution of the output light intensity after the signal is passed through a two-stage discrete sampling system. We

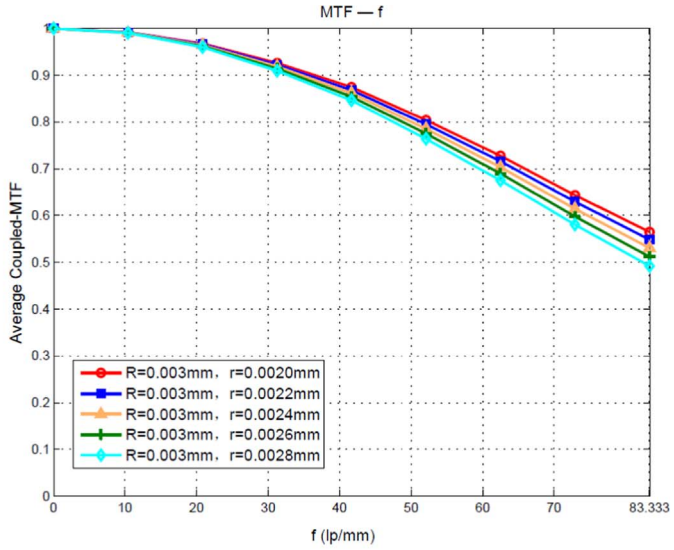

(a) Simulation curve of the average coupled-MTF with different core layer radii at cladding radius R=0.003 mm

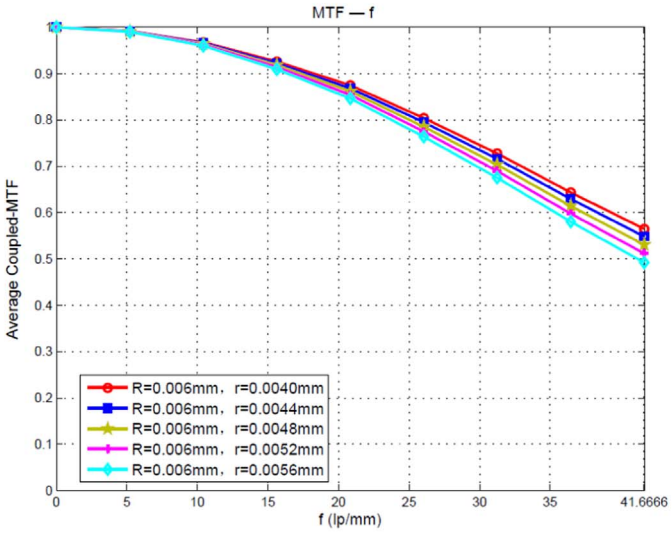

(b) Simulation curve of the average coupled-MTF with different core layer radius at cladding radii R=0.006 mm

Fig. 16. Average coupled-MTF curve in the Nyquist frequency domain under different cladding and core radius ratios. (a) Simulation curve of the average coupled-MTF with different core layer radii at cladding radius R=0.003 mm. (b) Simulation curve of the average coupled-MTF with different core layer radius at cladding radii R=0.006 mm.

Table 2
Relative changes in the value of average coupled-MTF with different cladding layers and core layer radius ratios.

(R-r)/R	R=0.003 mm	R=0.006 mm
33%	MTF(f_N)=0.5703	MTF(f_N)=0.5647
6.7%	MTF(f_N)=0.4981	MTF(f_N)=0.4921
	ΔMTF(f_N)=0.0722	ΔMTF(f_N)=0.0726

observed some new characters of coupled-MTF and its average by mathematical simulation and analysis as follows:

(1) In the presence of an extremely small deviation between the spatial frequency of the input signal and the Nyquist frequency, the coupled-MTF oscillation converges to fixed values followed with the number increasing of pixels in the array. The convergence rate of the coupled-MTF is related to spatial frequency deviation. A smaller deviation of the spatial frequency results in slower convergence rates of the coupled-MTF.
(2) The convergence properties of the coupled-MTF exist in the sagittal and tangential directions simultaneously, but the convergence value of two directions is related to pixel-coupled error. If the pixel-coupled errors in a system are different in sagittal and tangential directions separately, the deviation results in a different MTF value in the sagittal and tangential directions.
(3) The coupled-MTF periodically oscillates with the pixel-coupled error. The cycle of the oscillation is equal to the diameter of fiber cladding (or the core distance). The oscillation amplitude of the coupled-MTF is positively correlated to the deviation between the spatial frequency of the input signal and the Nyquist frequency. The amplitude of the coupled-MTF oscillation caused by the pixel coupling error is close to 0.5 when the deviation of the spatial frequency is 1%. These patterns are observed in the sagittal and tangential directions of the pixel array. The oscillation frequency and amplitude of the coupled-MTF in the sagittal and tangential directions are consistent.
(4) The alignment error between the grayscale cosine distribution signal and the coupled-pixel array affect the strictness of the transfer function evaluation model. In addition, random pixel-coupled error results in the oscillation of coupled-MTF. These issues are solved by defining the average coupled-MTF. Moreover, the average coupled-MTF can objectively evaluate the imaging performance of the two-level coupled discrete sampling image system in a manner consistent with the definition of the traditional MTF. The simulation results indicate that smaller distance between adjacent fiber cores generates higher MTF values for the coupled imaging system in the whole Nyquist frequency domain. Consequently, the cut-off frequency of the system is greatly improved. This greatly contribute to the improvement of the imaging ability of target details and contour resolution for optical imaging systems composed of array fiber-optic image bundles and CCD.
(5) The ratio of the optical fiber cladding layer to its core layer radius slightly affects the imaging quality of the system. For example, the MTF value in corresponding Nyquist frequency is only the variation of 0.07 when the ratio difference is five times. This result shows that cladding radius or distance between fiber cores should be determined in actual design processing based on the resolution and imaging quality. Then, the fiber core layer should be identified in accordance with the SNR of the system. However, the influence of the core layer radius on the MTF should be disregarded. For instance, the radius of the fiber core layer should be selected based onSNR, and the imaging quality should be considered based on the radius of the cladding in design processing in high-resolution hyperspectral applications.

The development of a test light path is underway. We also aim to report a comprehensive experimental verification of our theoretical analysis and mathematical simulation in our future work. The authors thank the National Scientific Fund of China (No. 61675198 and No. 61307114) for its financial support.

References

[1] Zhou Dechun, Yu Fengxia, Tan Fang, Preparation and optical performance of high resolution optical fiber image bundle, Chin. J. Lasers 36 (2011) 723–726.
[2] S. Inoue, T. Katagiri, Y. Matsuura, Fiber-optic direct Raman imaging system based on a hollow-core fiber bundle, Proc. SPIE 9317 (2015) (0V-1–0V-5).
[3] Stephen J. Olivas, Ashkan Arianpour, Igor Stamenov, Rick Morrison, Ron A. Stack, Adam R. Johnson, Ilya P. Agurok, Joseph E. Ford, Image processing for cameras with fiber bundle image relay, Appl. Opt. 54 (2015) 1124–1137.
[4] David William Fletcher-Holmes, Andrew Robert Harvey, A snapshot foveal hyperspectral imager, Proc. SPIE 4816 (2002) 407–414.
[5] Donald M. Chiarulli, Steven P. Levitan, Paige Derr, Robert Hofmann, Bryan Greiner, Matt Robinson, Demonstration of a multichannel optical interconnection by use of imaging fiber bundles butt coupled to optoelectronic circuits, Appl. Opt. 39 (2000) 698–703.
[6] A. Seki, K. Iwai, T. Katagiri, Y. Matsuura, Photoacoustic imaging by using a bundle of thin hollow-optical fibers, Proc. SPIE 9702 (2016) 970202-1–970202-6.
[7] Helen D. Ford, Ralph P. Tatam, Characterization of optical fiber imaging bundles for swept-source optical coherence tomography, Appl. Opt. 50 (2011) 627–640.
[8] Thomas Carter, Sampled MTF of fused fiber optic components and bonded assemblies, Proc. SPIE 8735 (2013) 07–1–07-5.
[9] S.E. Schacham, M.E. Marhic, C. Kot, M. Epstein, Coupling of rigid to flexible imaging multifibers, Appl. Opt. 17 (1978) 3818–3821.
[10] Renee Drougard, Optical transfer properties of fiber bundles, J. Opt. Soc. Am. 54 (1964) 907–914.
[11] Lin Huang, Ulf Österberg, Measurement of crosstalk in order-packed image fiber bundles, Proc. SPIE 2536 (1995) 480–488.
[12] Ikhlef Abdelaziz, Maurice Skowronek, Application of a plastic scintillating fiber array for low-energy x-ray imaging, Appl. Opt. 37 (1998) 8081–8084.
[13] Jae-Ho Han, Junghoon Lee, Jin U. Kang, Pixelation effect removal from fiber bundle probe based optical coherence tomography imaging, Opt. Express 18 (2010) 7427–7439.
[14] Xu He, Yang Xiang, Study on a method of evaluating the alignment of pixels between fiber-optic image bundles and detector arrays, Appl. Opt. 50 (E189–E192) (2011).
[15] Hong Minfang, Shen Jianqi, Zhang Qiuchang, Yu Bin, Propagation of Gaussian beam through planar interface, Chin. J. Lasers 38 (7) (2011) 1–5.
[16] Zang Liuqing, Zhang Zhenxi, Miao Baogang, peng Niancai, Li Zheng, Multiclor fluorescence detection in the multiplex quantitative PCR system and spectra crosstalk correction method, Acta Opt. Sin. 34 (1) (2014) 1–7.
[17] John B. Kiser, Brian, M. Cullum, Optical crosstalk and surface characterization of SERS nanoimaging bundle substrates, Proc. SPIE 7674 (2010) 1–8.